

## **A digital microfluidic platform based on a near-infrared light-responsive shape-memory micropillar array**

Wen-Qi Ye, Yun-Yun Wei, Dan-Ni Wang, Chun-Guang Yang, Zhang-Run Xu\*

*Research Center for Analytical Sciences, Northeastern University, Shenyang, 110819, China.*

\*Corresponding author: Tel.: +86-24-83687659; E-mail: xuzr@mail.neu.edu.cn.

### **Experimental**

#### **Materials and reagents**

EVA (containing 18 wt.% vinyl acetate) and hexadecyl trimethyl ammonium bromide (CTAB,  $\geq 99.0\%$ ) were purchased from Macklin Co., Ltd. (Shanghai, China). 5-bromosalicylic acid (5-BrSA) and 1,1,1,3,3,3-hexamethyldisilazane (HMDS) were purchased from Aladdin Chemical Reagent Co., Ltd. (Shanghai, China). Dicumyl peroxide (DCP), Chloroauric Acid ( $\text{HAuCl}_4 \cdot 4\text{H}_2\text{O}$ ), sodium borohydride ( $\text{NaBH}_4$ ), silver nitrate ( $\text{AgNO}_3$ ), thioglycolic acid, toluene, tetrahydrofuran, ascorbic acid, and methanol were obtained from Sinopharm Chemical Reagent Co., Ltd. (Shenyang, China). Hexadecane was purchased from TCI Co., Ltd. (Shanghai, China). The water used in the experiment is deionized water.

#### **Synthesis of AuNRs**

AuNRs were prepared according to the seed growth method in the literature.<sup>1</sup> The preparation method of gold seed aqueous solution is consistent with that in the literature reported by our group.<sup>2</sup> For synthesizing the growth solution, 4.5 g of CTAB and 0.55 g of 5-BrSA were dissolved in 125 mL of water at 70°C. After the solution was cooled to 30°C, 8 mL (4 mM) of  $\text{AgNO}_3$

solution was added, and the solution stood for 15 min. 4.25 mL (25 mM) of chloroauric acid stock solution was diluted to 125 mL, and then added into the mixed solution, stirred (400 rpm) for 15 min. 1 mL (64 mM) of ascorbic acid was added and stirred violently for 30 s until the solution became colorless. 0.4 mL seed solution was added to the growth solution, and the reaction was carried out in a water bath at 30°C for 12 h. The synthesized AuNRs solution was centrifuged for 25 min at 11000 rpm, and the supernatant was removed. The above operation was repeated twice.

### **Preparation of EVA composite sample**

Synthesis of EVSH based on thiol substitution methods was reported by previous reports.<sup>3, 4</sup> In short, EVA was partially hydrolyzed in alcoholic sodium hydroxide solution and reacted with thioglycolic acid to contain thioglycolic groups. 0.1 g of EVSH was added to 30 mL of tetrahydrofuran and stirred to dissolve at 50°C. 30 mL AuNRs solution was added and reacted for 10 min. Then 30 mL of toluene at 50°C was added to extract the organic phase. 30 mL of organic phase solution (EVS-AuNRs, 1.16 mg mL<sup>-1</sup>) was mixed with 20 mL of toluene, and heated to 80 °C in water bath. Then 3.0 g of EVA and 0.075 g of DCP were added and stirred until dissolved. The solution was poured into a glass petri dish with a cover and cooled to room temperature. After the EVA composite solidified, it was put in a vacuum drying oven and dried to constant weight at 35 °C. The EVA composite contains 96.3 % EVA, 2.5 % DCP and 1.2 % EVS-AuNRs. EVA composite samples were pressed on a heating plate at 80°C to obtain samples with smooth surface.

### **Characterization of EVS-AuNRs and EVA composite**

Thermogravimetric analysis (TGA) was performed to measure the weight fraction of AuNRs on a thermogravimetric analyzer (Mettler Toledo, Switzerland) from 25°C to 700°C at 10°C min<sup>-1</sup> under a nitrogen flow of 40 mL min<sup>-1</sup>. The result shows that the weight fraction of AuNRs in

EVS-AuNRs is 1.33% (Fig. S1).

The EVA composite was characterized by using differential scanning calorimetry (DSC). Under nitrogen flow ( $50 \text{ mL min}^{-1}$ ), the first heating is from  $25^\circ\text{C}$  to  $100^\circ\text{C}$  at  $10^\circ\text{C min}^{-1}$ , the first cooling is from  $100^\circ\text{C}$  to  $25^\circ\text{C}$  at  $5^\circ\text{C min}^{-1}$ , and the second heating is from  $25^\circ\text{C}$  to  $100^\circ\text{C}$  at  $5^\circ\text{C min}^{-1}$ . As shown in Fig. S3, the cooling curve indicates that EVA composite has an exothermic peak at  $50.3^\circ\text{C}$  (crystallization temperature). We confirmed that the transition temperature was about  $52^\circ\text{C}$  by observing the shape recovery of EVA in water bath. The crystallization temperature is almost consistent with the transition temperature.

X-ray photoelectron spectroscopy (XPS) was measured to characterize Au-S bonds in EVS-AuNRs. In Fig. S4, there are two peaks at  $84.4 \text{ eV}$  and  $88.1 \text{ eV}$ , which are consistent with the binding energies of  $\text{Au } 4f_{7/2}$  and  $\text{Au } 4f_{5/2}$ , indicating that Au-S bonds are formed on the AuNRs.

We used a high-speed camera to take photos of droplets on the micropillar array in original shape and temporary shape. As shown in Fig. S5, the droplet is in Cassie state. The reason for this phenomenon is that the micropillar array is completely immersed in hexadecane. Because hexadecane has better affinity to EVA composite, the droplet will not wet micropillar surface.

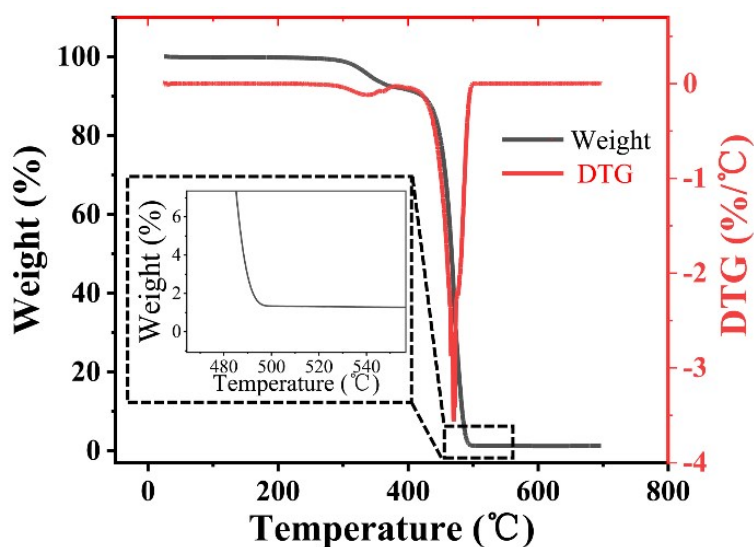


Fig. S1 TGA and derivative thermogravimetry (DTG) curves of EVS-AuNRs

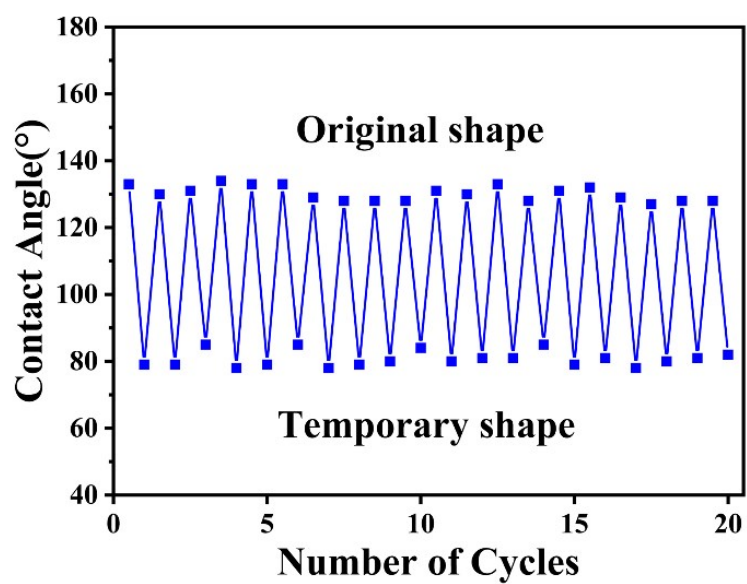


Fig. S2 Contact angles of the micropillar array repeatedly pressed and recovered for twenty times.

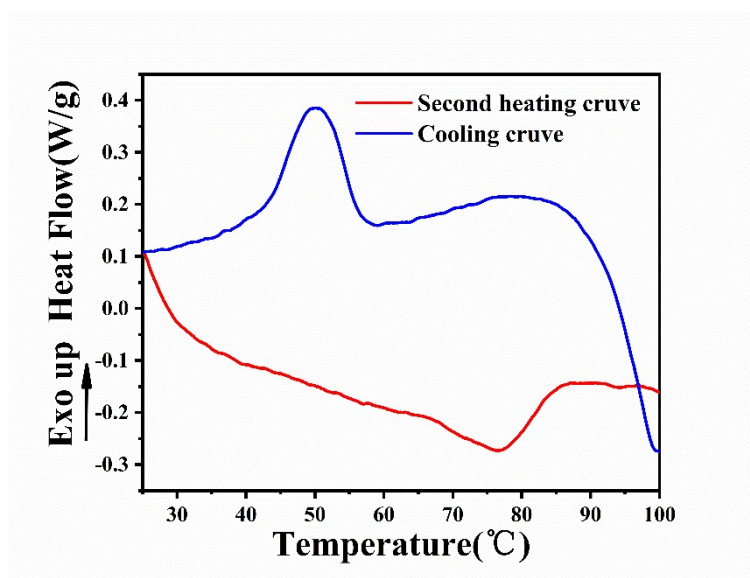


Fig. S3 DSC second heating and cooling curves of crosslinked EVA composite.

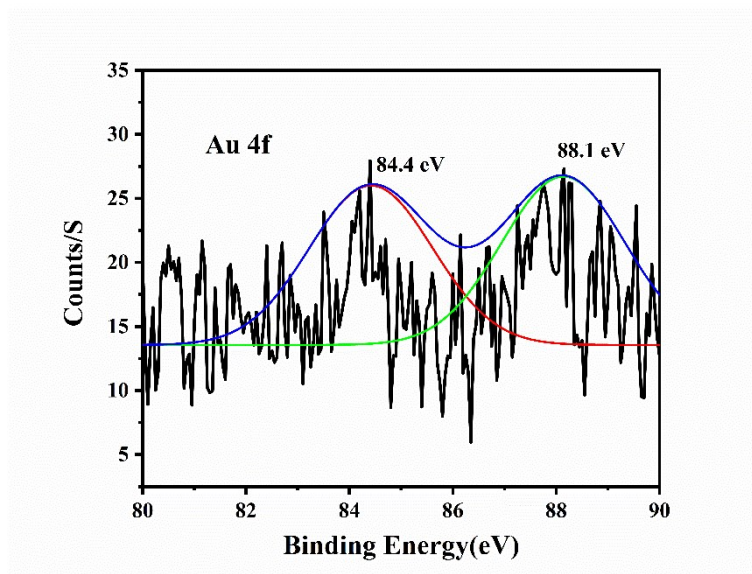


Fig. S4 Au 4f XPS spectrum of the EVS-AuNRs.

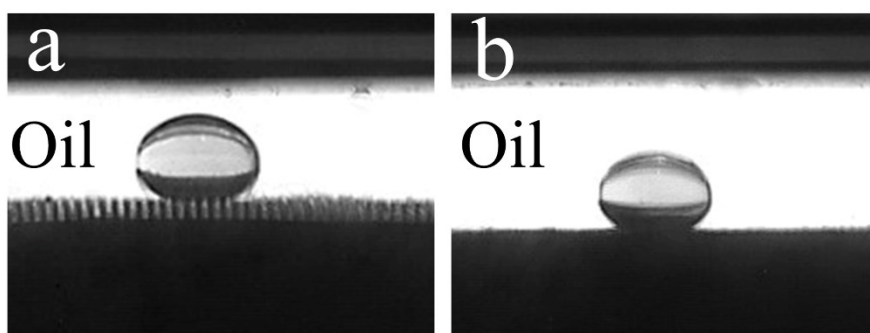


Fig. S5 Photographs of the droplet on the micropillar array in original shape (a) and in temporary shape (b).

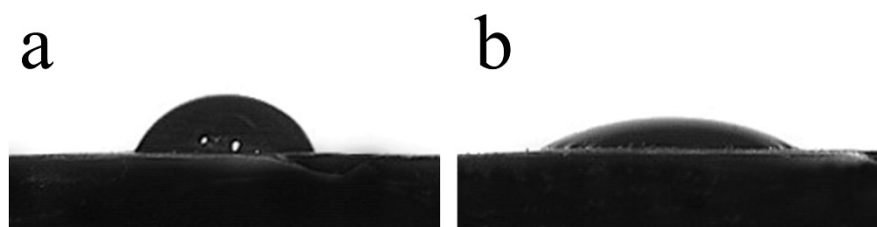


Fig. S6 Droplets of water (a) and hexadecane (b) on EVA composite surface.

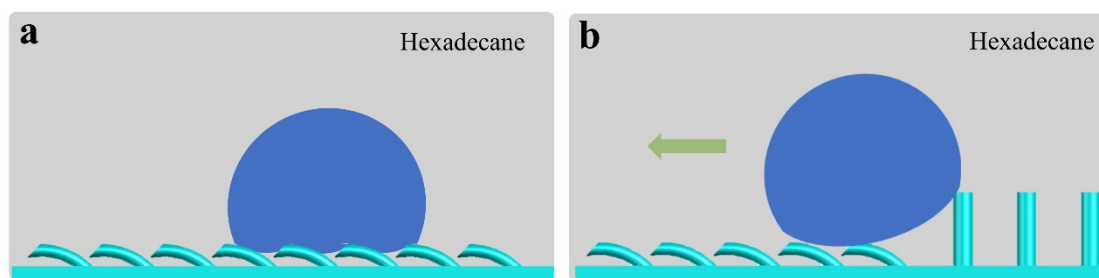


Fig. S7 Schematics of droplet on the micropillar array in temporary shape (a) and droplet driven to the left (b).

### Supporting videos

Video S1: A blue droplet moving in a straight line and merging with a red droplet.

Video S2: A 2- $\mu\text{L}$  droplet moving in an N-shaped path.

Video S3: Movement and fusion of a 0.1- $\mu\text{L}$  droplet and a 10- $\mu\text{L}$  droplet.

### Reference

1. X. Ye, L. Jin, H. Caglayan, J. Chen, G. Xing, C. Zheng, V. Doan-Nguyen, Y. Kang, N. Engheta, C. R. Kagan and C. B. Murray, *ACS Nano*, 2012, **6**, 2804-2817.
2. D. Wang, R. Guo, Y. Wei, Y. Zhang, X. Zhao and Z. Xu, *Biosens Bioelectron*, 2018, **122**, 247-253.
3. F. Ge, X. Lu, J. Xiang, X. Tong and Y. Zhao, *Angew Chem Int Ed Engl*, 2017, **56**, 6126-6130.
4. M. Tang, J. Hou, L. Lei, X. Liu, S. Guo, Z. Wang and K. Chen, *Int J Pharm*, 2010, **400**, 66-73.
5. H. Zhu, M. Du, M. Zhang, P. Wang, S. Bao, M. Zou, Y. Fu and J. Yao, *Biosens Bioelectron*, 2014, **54**, 91-101.